Behavior of High-Pressure Air in Critical-Flow Through Nozzles

Bruno Schmidt,* Richard Martin,† and Clifford House‡
Southwest Missouri State University, Springfield, Missouri 65804

This paper reports mass flux for air in critical-flow through nozzles that have been calculated using a fundamental equation for air expressed in terms of the Helmholz energy. Flux values are reported for plenum pressures up to 3.4×10^7 N/m^2, and temperatures that range from 225 K to 800 K. Critical flow factors are also reported for this pressure and temperature range. The results agree very well with those previously calculated for lower pressures, and whose values have been well established experimentally. The present results represent an extension of critical flow factors to much higher plenum pressures and temperatures.

Nomenclature

A = Helmholt energy, J/kg
a = sonic velocity, m/s
C^* = dimensionless critical flow factor
C_v = specific heat at constant volume, J/kg·K
C_p^0 = ideal specific heat at constant pressure, J/kg·K
G_i = empirical parameters in equation of state, K^{4-i}, $1\le i\le 7$
G_8 = empirical parameter in equation of state (dimensionless)
G_9 = empirical parameter in equation of state, K
H_0^0 = reference value for enthalpy (at $P=1.01325\times10^5$ N/m^2 and $T=298.15$ K)
i,j,ℓ = dimensionless empirical parameters in equation of state
N_k = dimensionless coefficients in equation of state
P = pressure, N/m^2
R = gas constant for air, J/kg·K
S = entropy, J/kg·K
S_0^0 = reference value for entropy (at $P=1.01325\times10^5$ N/m^2 and $T=298.15$ K)
T = temperature, K
T_m = temperature at maxcondentherm, K
u = dimensionless parameter in equation of state, G_9/T
V = velocity, m/s
W = mass flux, kg/m^2·s
α = "nondimensional" Helmholt energy, $A/(RT)$
α^0 = ideal gas contribution to α
$\bar{\alpha}$ = real gas contribution to α
δ = dimensionless reduced density, ρ/ρ_m
δ_0 = dimensionless reduced reference density (at $P=1.01325\times10^5$ N/m^2 and $T=298.15$ K)
γ = dimensionless parameter in equation of state
ρ = density, kg/m^3
ρ_m = density at maxcondentherm, kg/m^3
τ = dimensionless reduced temperature, T_m/T
τ_0 = dimensionless reduced reference temperature (at $P=1.01325\times10^5$ N/m^2 and $T=298.15$ K)

Subscripts

n = nozzle conditions
p = plenum conditions

Received June 30, 1988; revision received Oct. 18, 1988.

*Professor, Computer Science Department.
†Instructor, Computer Science Department.
‡Associate Professor, Industrial Technology Department.

Introduction

ROBERT C. Johnson[1] calculated the mass flow rates for air in critical-flow through nozzles for plenum temperatures ranging from 400°R to 700°R (222 K to 389 K) and plenum pressures up to 100 atm (1.01325×10^7 N/m^2). He tabulated his results in terms of the critical flow factor C^*, defined as

$$C^* = \rho_n V_n \sqrt{RT_p}/P_p \tag{1}$$

Under choked conditions, V_n is the sonic velocity. Further, the flow from the plenum to nozzle is assumed to be reversible and isentropic.

With these assumptions, any thermodynamic path of integration using pressure and temperature—P_p, T_p, to P_n, T_n—or density and temperature—ρ_p, T_p to ρ_n, T_n—should yield the same field state variables entropy S_n and velocity V_n. In particular, the entropy should not change, and the velocity should be sonic. Johnson chose a convenient integration path and used an empirical equation of state to obtain final values of ρ_n and T_n for given P_p and T_p values. Those final values of ρ_n and T_n were iteratively adjusted to yield isentropic, sonic flow at the nozzle.

Since then, newer thermodynamic data for air have recently been used[2] in developing an empirical fundamental equation for air involving the Helmholz energy (much different than the equation of state used by Johnson), and which spans a much wider range of temperatures and pressures. This paper reports the results of manipulating the new fundamental equation to allow iterative techniques, similar to those of Johnson's, to yield critical flow factors for higher plenum pressures and temperatures. C^* has been found from Eq. (1) and tabulated for P_p ranging from 1.0×10^4 N/m^2 to 3.4×10^7 N/m^2 and T_p ranging from 225 K to 800 K.

With the table of C^* values for different P_p and T_p, it is possible to easily obtain the mass flux W from Eq. (1):

$$W = \rho_n V_n \tag{2a}$$

$$W = C^* P_p/\sqrt{RT_p} \tag{2b}$$

Integration of the Equation of State

The thermodynamic path that has been chosen involves a change in temperature from T_p to T_n (at constant density ρ_p) followed by a change in density from ρ_p to ρ_n (at constant temperature T_n). The underlying relationships that lead to integrable expressions for S and V are[1] the expression for differential entropy

$$dS = C_v dT/T - (\partial P/\partial T)_\rho d\rho/\rho^2 \tag{3}$$

the expression for differential enthalpy

$$dH = TdS + Pd\rho/\rho^2 + d(P/\rho) \tag{4}$$

and the energy equation

$$dH = -VdV \tag{5}$$

Combining Eqs. (4) and (5) yields

$$-VdV = TdS + Pd\rho/\rho^2 + d(P/\rho) \tag{6}$$

To be able to perform the integrations of Eqs. (3) and (6), it was found convenient to express the thermodynamic variables in terms of the Helmholtz Energy A. A, in turn, can be written as a nondimensional function $\alpha(\delta,\tau)$, which is the fundamental equation mentioned in the introduction:

$$\alpha(\delta,\tau) = A(\rho,T)/RT = \alpha^0(\delta,\tau) + \bar{\alpha}(\delta,\tau) \tag{7}$$

This can be written using

$$A = U - TS = H - RT - TS \tag{8}$$

and so

$$A/RT = H/RT - 1 - S/R \tag{9}$$

Using the differential forms for enthalpy and entropy

$$dH = C_p dT \tag{10}$$

$$dS = C_p dT/T - R dP/P \tag{11}$$

we can combine Eqs. (7), (9), (10), and (11), and integrate to finally express the ideal gas contribution as

$$\alpha^0(\delta,\tau) = H_0^0\tau/(RT_m) - S_0^0/R - 1 + \ell n[(\delta\tau_0)/(\delta_0\tau)] - (\rho/R)\int_{\tau_0}^{\tau}(C_p^0/\tau^2)\,d\tau + (1/R)\int_{\tau_0}^{\tau}(C_p^0/\tau)\,d\tau \tag{12}$$

Further, an empirical expression for the ideal gas heat capacity is taken to be[2]

$$C_p^0/R = \sum_{i=1}^{7} G_i T^{i-4} + G_8\,[u^2e^u/(e^u-1)^2] \tag{13}$$

with $u = G_9/T$.

An empirical expression for the real gas contribution is[2]

$$\bar{\alpha}(\delta,\tau) = \sum_{k=1}^{28} N_k \delta^i \tau^j \exp(-\gamma\delta^\ell) \tag{14}$$

The above fundamental equation relationships are described in more detail in Ref. 2, along with the numerical techniques for obtaining N_k, i, j, δ, ℓ, and G_i. Revised empirical values of N_k, i, j, γ, δ, ℓ, and G_i have since been reported,[3] and have been used in this work. They are reproduced in Tables 1 and 2. Values for ρ_m and R used in this paper are 302.62 kg/m^3 and 287.11 J/(kg · K), respectively, and are based upon the following values[2]: an assumed air composition that is 78.14 mole percent N_2, 20.93 mole percent O_2, and 0.93 mole percent Ar, a maxcondotherm density ρ_m of 10.45 mole/dm^3, and a gas constant R equal to 0.00831434 (MPa · dm^3)/(mol · K). Also,[2] T_m is 132.6639 K.

To integrate Eqs. (3) and (6) using the Helmholz Energy and the parameters of Tables 1 and 2, three other thermodynamic relationships have been used:

$$C_v = T(\partial S/\partial T)_v \tag{15}$$

$$S = -(\partial A/\partial T)_v \tag{16}$$

$$P = \rho^2(\partial A/\partial\rho)_T \tag{17}$$

Integrating Eq. (3) and using Eqs. (7) and (12–17) we obtain

$$\frac{\Delta S}{R} = -\ell n\left(\frac{\delta_n T_n}{\delta_p T_p}\right) + \sum_{\substack{i=1\\ \neq 4}}^{7} G_i\left(\frac{T_n^{i-4} - T_p^{i-4}}{i-4}\right) + G_4\,\ell n\left(\frac{T_n}{T_p}\right) + G_8\left[\frac{u_n e^{u_n}}{e^{u_n}-1} - \frac{u_p e^{u_p}}{e^{u_p}-1} - \ell n\left(\frac{e^{u_n}-1}{e^{u_p}-1}\right)\right] + \sum_{k=1}^{28} N_k(j-1)\{\tau_n^j\,[1+\delta_n^i\exp(-\gamma\delta_n^\ell) - \delta_p^i\exp(-\gamma\delta_p^\ell)] - \tau_p^j\exp(-\gamma\delta_p^\ell)\} \tag{18}$$

Integrating Eq. (6) with the aid of Eqs. (7), (12–14), (16), and (17),

$$V_n^2 = 2R\Bigg\{-\sum_{\substack{i=1\\ \neq 3}}^{7} G_i(T_n^{i-3} - T_p^{i-3})/(i-3) - G_3\ell n(T_n/T_p) - G_8G_9\,[1/(e^{u_n}-1) - 1/(e^{u_p}-1)] - \sum_{k=1}^{28} N_k\,[\tau_n^j T_n\delta_n^i\,(i+j-\gamma\ell\delta_n^{\ell-1})\exp(-\gamma\delta_n^\ell) - \tau_p^j T_p\delta_p^i\,(i+j-\gamma\ell\delta_p^{\ell-1})\exp(-\gamma\delta_p^\ell)]\Bigg\} \tag{19}$$

Table 1 Parameters G_i for C_p^0

i	G_i
1	35141.99501
2	−1384.757143
3	19.10646293
4	3.381739067
5	$0.2233060919\times10^{-3}$
6	0.0
7	$-0.2034304300\times10^{-10}$
8	0.7793261063
9	3089.00000

Table 2 Parameters for $\bar{\alpha}$

k	N_k	i	j	γ	ℓ
1	0.05818435365	1	0.00	0	0
2	1.736326963	1	0.50	0	0
3	−3.911954826	1	1.00	0	0
4	1.223875677	1	1.25	0	0
5	0.02206697573	2	−.50	0	0
6	0.2588481315	2	1.50	0	0
7	−.1509953670	2	2.00	0	0
8	−.06402079838	3	0.00	0	0
9	0.1086937989	3	0.25	0	0
10	−.08631420022	3	1.00	0	0
11	0.01378013032	4	0.25	0	0
12	−.0001329965612	6	0.00	0	0
13	0.0004593125113	7	2.00	0	0
14	0.000001000804929	7	5.00	0	0
15	−.00009764062170	8	2.00	0	0
16	−.2124354978	1	5.00	1	2
17	0.08772223864	1	6.00	1	2
18	0.02329240620	2	5.50	1	2
19	−.04554544968	3	7.00	1	2
20	0.02312505921	4	0.50	1	2
21	−.03215216273	4	1.50	1	2
22	−.0002665115250	6	8.50	1	2
23	0.006525277882	7	4.00	1	2
24	0.0003133766347	10	5.50	1	2
25	−.01245547044	4	23.00	1	4
26	0.009471289032	5	18.00	1	4
27	0.008669574209	8	0.50	1	2
28	−.01039549880	8	1.00	1	2

An alternate way to calculate sonic velocity is to use

$$a^2 = (\partial P/\partial \rho)_s \tag{20}$$

Combining Eq. (20) with Eq. (17) and using Eqs. (7), (12–14) produce an empirical expression for the sonic velocity as a state variable:

$$a^2 = RT + RT\sum_{k=1}^{28} f[i^2 - \gamma\ell(2i + \ell)\delta^\ell + \gamma^2\ell^2\delta^{2\ell}] - RT\left\{1 - \sum_{k=1}^{28} f(j-1)(i - \gamma\ell\delta^\ell)\right\}^2 \Bigg/ \left\{1 - \sum_{i=1}^{7} G_i T^{i-4} - G_8 \frac{u^2 e^u}{(e^u-1)^2} + \sum_{k=1}^{28} f_{ijk\ell} j(j-1)\right\} \tag{21}$$

with

$$f = \delta^i \tau^j N_k \exp(-\gamma\delta^\ell) \tag{22}$$

Equation (17) can be used to explicitly relate pressure to density (or to δ). This is necessary because it is customary to specify a plenum pressure from which the density (and δ) must be obtained, as entropy and velocity have been expressed in terms of temperature and density, not temperature and pressure. Equation (17) yields

$$P = \rho RT\left[1 + \sum_{k=1}^{28} N_k \tau^j \delta^i (i - \gamma\ell\delta^\ell)\exp(-\gamma\delta^\ell)\right] \tag{23}$$

Numerical Techniques

Step 1. Given a plenum pressure and temperature P_p and T_p, δ_p is adjusted so that P from Eq. (23) satisfies the condition $|P - P_p| < 10^{-4} P_p$. Because P is a monotonically increasing function of δ and is very well behaved, convergence is obtained quickly. The initial estimate for δ_p is based on the ideal gas assumption

$$\delta = P/(\rho_m \cdot R \cdot T) \tag{24}$$

Step 2. Next, the nozzle density and temperature are estimated from the ideal gas approximation yielding first approximations of

$$T_n = T_p/1.2 \tag{25}$$

and

$$\rho_n = \rho_p(1/1.2)^{2.5} \tag{26}$$

Step 3. As expected from an ideal gas analysis, sonic velocity varies only slowly with density. On the other hand, V_n from Eq. (19) increases with decreasing T_n, while sonic velocity a from Eq. (21) increases with increasing T_n. Thus, the estimate of T_n is improved upon by varying T_n until $|a - V_n|$ is acceptably close to zero, which is

$$|a - V_n| < 10^{-3} \text{ m/s} \tag{27}$$

Step 4. Following this, ρ_n is adjusted from the ideal gas approximation until the entropy change ΔS from Eq. (18) is acceptably close to zero, which is

$$|\Delta S| < 10^{-5} R \tag{28}$$

With a new value of ρ_n, steps 3 and 4 are repeated a sufficient number of times to satisfy both numerical conditions Eqs. (27) and (28) for the same ρ_n and T_n.

Discussion of Results

The Critical Factor C^* for pressures of 1×10^7 N/m^2 (100 atm) or lower is displayed in Table 3. For low pressures, the results agree very well with those of Johnson.[1] At pressures lower than 5×10^6 N/m^2, differences are always less than 0.1%. At higher pressures, the differences become more pronounced in the lower temperature region of the calculations. For instance, at 1×10^7 N/m^2, the discrepancy exceeds 0.1% for plenum temperatures below 275 K, and exceeds 0.5% at 225 K. A comparison of the two results is displayed in Fig. 1.

Table 3 C^* at low pressures

	Plenum pressure $\times 10^{-5}$, N/m^2										
T(K)	1	10	20	30	40	50	60	70	80	90	100
225	0.6856	0.6918	0.6987	0.7060	0.7134	0.7210	0.7287	0.7365	0.7442	0.7519	0.7594
250	0.6854	0.6898	0.6948	0.6999	0.7050	0.7101	0.7153	0.7204	0.7254	0.7303	0.7352
275	0.6852	0.6885	0.6921	0.6957	0.6993	0.7030	0.7065	0.7100	0.7135	0.7169	0.7201
300	0.6851	0.6875	0.6901	0.6928	0.6954	0.6980	0.7005	0.7030	0.7054	0.7078	0.7101
325	0.6849	0.6867	0.6887	0.6906	0.6925	0.6944	0.6962	0.6980	0.6997	0.7014	0.7030
350	0.6848	0.6861	0.6875	0.6890	0.6904	0.6917	0.6930	0.6943	0.6955	0.6967	0.6978
375	0.6846	0.6856	0.6866	0.6877	0.6887	0.6896	0.6905	0.6914	0.6923	0.6931	0.6938
400	0.6844	0.6851	0.6858	0.6866	0.6873	0.6879	0.6886	0.6892	0.6898	0.6903	0.6908
425	0.6841	0.6846	0.6851	0.6856	0.6861	0.6866	0.6870	0.6874	0.6877	0.6881	0.6884
450	0.6839	0.6842	0.6845	0.6848	0.6851	0.6854	0.6856	0.6859	0.6861	0.6862	0.6864
475	0.6836	0.6837	0.6839	0.6841	0.6842	0.6844	0.6845	0.6846	0.6847	0.6847	0.6847
500	0.6832	0.6833	0.6834	0.6834	0.6834	0.6835	0.6835	0.6835	0.6834	0.6834	0.6833
525	0.6829	0.6829	0.6828	0.6828	0.6827	0.6827	0.6326	0.6825	0.6824	0.6822	0.6821
550	0.6825	0.6824	0.6823	0.6822	0.6820	0.6819	0.6817	0.6816	0.6814	0.6812	0.6810
575	0.6821	0.6819	0.6817	0.6816	0.6814	0.6812	0.6810	0.6808	0.6805	0.6803	0.6800
600	0.6816	0.6815	0.6812	0.6810	0.6808	0.6805	0.6803	0.6800	0.6797	0.6794	0.6791
625	0.6812	0.6810	0.6807	0.6804	0.6802	0.6799	0.6796	0.6793	0.6790	0.6787	0.6783
650	0.6807	0.6805	0.6802	0.6799	0.6796	0.6793	0.6789	0.6786	0.6783	0.6779	0.6776
675	0.6803	0.6800	0.6797	0.6794	0.6790	0.6787	0.6783	0.6780	0.6776	0.6773	0.6769
700	0.6798	0.6795	0.6792	0.6788	0.6785	0.6781	0.6778	0.6774	0.6770	0.6766	0.6762
725	0.6794	0.6791	0.6787	0.6783	0.6780	0.6776	0.6772	0.6768	0.6764	0.6760	0.6756
750	0.6789	0.6786	0.6782	0.6778	0.6775	0.6771	0.6767	0.6763	0.6759	0.6755	0.6751
775	0.6785	0.6781	0.6777	0.6773	0.6770	0.6766	0.6762	0.6758	0.6754	0.6749	0.6745
800	0.6780	0.6777	0.6773	0.6769	0.6765	0.6761	0.6757	0.6753	0.6748	0.6744	0.6740

Table 4 C^* at high pressures

	Plenum pressure × 10^{-5}, N/m^2											
T(K)	120	140	160	180	200	220	240	260	280	300	320	340
225	0.7737	0.7868	0.7988	0.8092	0.8181	0.8255	0.8313	0.8357	0.8386	0.8403	0.8407	0.8402
250	0.7444	0.7530	0.7607	0.7675	0.7735	0.7786	0.7828	0.7861	0.7886	0.7904	0.7915	0.7920
275	0.7264	0.7322	0.7373	0.7419	0.7460	0.7494	0.7523	0.7546	0.7565	0.7579	0.7588	0.7593
300	0.7144	0.7183	0.7219	0.7250	0.7278	0.7301	0.7320	0.7336	0.7348	0.7357	0.7363	0.7366
325	0.7060	0.7087	0.7111	0.7133	0.7151	0.7166	0.7179	0.7189	0.7196	0.7201	0.7204	0.7204
350	0.6999	0.7018	0.7034	0.7048	0.7060	0.7069	0.7077	0.7082	0.7086	0.7088	0.7088	0.7086
375	0.6953	0.6965	0.6976	0.6985	0.6992	0.6997	0.7001	0.7003	0.7004	0.7003	0.7001	0.6998
400	0.6917	0.6925	0.6931	0.6936	0.6940	0.6942	0.6943	0.6942	0.6941	0.6938	0.6934	0.6930
425	0.6889	0.6893	0.6896	0.6898	0.6899	0.6899	0.6897	0.6895	0.6892	0.6888	0.6883	0.6877
450	0.6866	0.6868	0.6868	0.6868	0.6867	0.6864	0.6861	0.6857	0.6853	0.6847	0.6841	0.6835
475	0.6847	0.6847	0.6845	0.6843	0.6840	0.6836	0.6832	0.6827	0.6821	0.6815	0.6808	0.6801
500	0.6831	0.6829	0.6826	0.6823	0.6818	0.6813	0.6808	0.6802	0.6795	0.6788	0.6781	0.6773
525	0.6818	0.6814	0.6810	0.6805	0.6800	0.6794	0.6788	0.6781	0.6774	0.6766	0.6758	0.6750
550	0.6806	0.6801	0.6796	0.6790	0.6784	0.6777	0.6770	0.6763	0.6755	0.6748	0.6739	0.6731
575	0.6795	0.6789	0.6783	0.6777	0.6770	0.6763	0.6756	0.6748	0.6740	0.6732	0.6723	0.6714
600	0.6786	0.6779	0.6773	0.6765	0.6758	0.6751	0.6743	0.6735	0.6726	0.6718	0.6709	0.6700
625	0.6777	0.6770	0.6763	0.6755	0.6748	0.6740	0.6732	0.6723	0.6715	0.6706	0.6697	0.6688
650	0.6769	0.6762	0.6754	0.6746	0.6738	0.6730	0.6722	0.6713	0.6704	0.6696	0.6687	0.6678
675	0.6762	0.6754	0.6746	0.6738	0.6730	0.6721	0.6713	0.6704	0.6695	0.6686	0.6677	0.6668
700	0.6755	0.6747	0.6739	0.6730	0.6722	0.6714	0.6705	0.6696	0.6687	0.6678	0.6669	0.6660
725	0.6748	0.6740	0.6732	0.6724	0.6715	0.6707	0.6698	0.6689	0.6680	0.6671	0.6662	0.6653
750	0.6743	0.6734	0.6726	0.6717	0.6709	0.6700	0.6691	0.6682	0.6673	0.6664	0.6655	0.6646
775	0.6737	0.6729	0.6720	0.6712	0.6703	0.6694	0.6685	0.6676	0.6667	0.6658	0.6649	0.6640
800	0.6732	0.6723	0.6715	0.6706	0.6697	0.6689	0.6680	0.6671	0.6662	0.6653	0.6644	0.6635

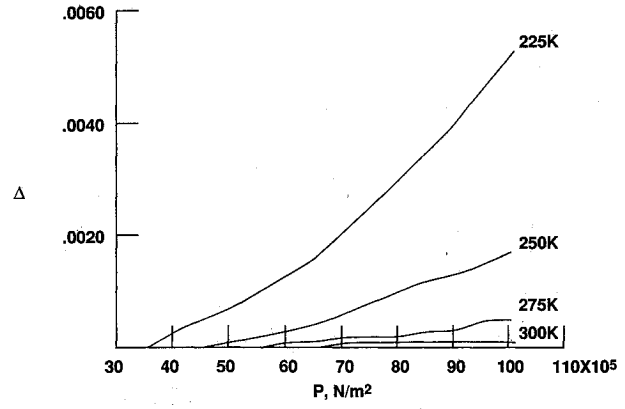

Fig. 1 Comparisons of critical factor values, $\Delta = C^*$ (previous results), $-C^*$ (present results).

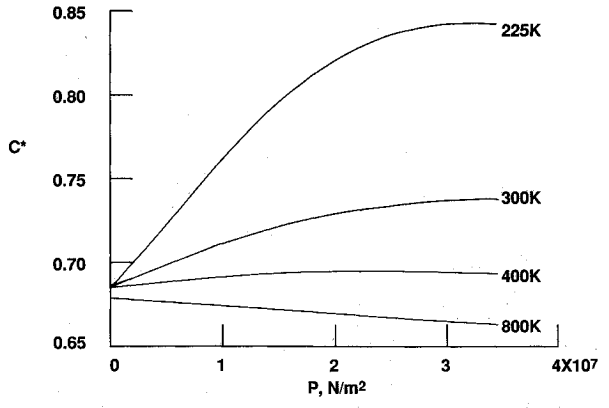

Fig. 2 Pressure behavior of the critical factor at selected temperatures.

The graph of Fig. 1 uses pressures expressed in N/m^2 for consistency. However, the comparisons of critical factors on that graph were made at pressure increments of $5 \times 1.01325 \times 10^5$ N/m^2 (5 atm) so that Johnson's original C^* values, tabulated in 5-atm increments, could be used.

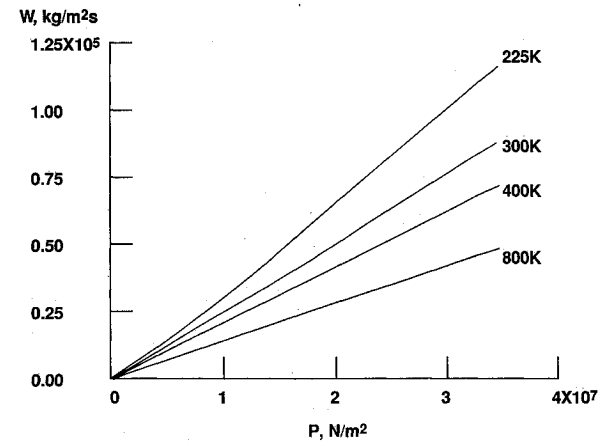

Fig. 3 Pressure behavior of the mass flux at selected temperatures.

Although the validity of Johnson's data has been well established experimentally for most plenum temperatures, it is in the very area of our discrepancy, where condensation at the nozzle is about to occur, that experimental verification is not available. Lacking that, we are confident that our low temperature/high-pressure values for C^* are more reliable than those used previously, for four reasons:

1) The analysis has been based upon more recent and reliable thermodynamic data.[4–8]

2) Particular attention was paid to obtaining equation of state parameters that are correct in the condensation region.[2]

3) The fundamental equation used here is based upon curve-fitting techniques that are more sophisticated, with many more tems, than what was used to obtain the earlier values of C^*.[1,2]

4) The original entropy and enthalpy Eqs. (3) and (4) can be written with specific heat in the dT term and compressibility in the $d\rho$ term. Johnson used an empirical expression for heat capacity that is useful only at low presssures.[1] This required that his path of integration be at low pressures whenever the temperature was changed. On the other hand, in using the fundamental equation in the Helmholtz energy in the present work, heat capacity parameters are found in both the dT and

$d\rho$ terms. Several integration paths were tested, both at low and high pressures when the temperature was changed. There was total self-consistency. All paths yielded the same value of C^* to four significant digits.

An absolute measurement of C^* would provide experimental verification. This could be accomplished by using a small container for the source of air. Its mass could be measured before and after a critical flow process, permitting W (and hence C^*) to be absolutely determined.

High-pressure values for C^* are given in Table 4, and the overall pressure behavior of C^* at selected temperatures is displayed in Fig. 2. It can be seen from Fig. 2 that at higher temperatures, C^* is a decreasing function of pressure, and at lower temperatures its pressure dependence exhibits a maximum. Yet W, calculated from Eq. (2b), always increases with pressure, as expected. This behavior is shown in Fig. 3.

More detailed tabulations of C^* than those reported here are available from the authors, as well as the FORTRAN source code that generated the results.

Acknowledgments

The authors wish to express their appreciation to the staff at McDonnell Douglas in St. Louis, including John Wynn, Alan Frazier, and Roger Crites in particular, for suggesting this problem and providing considerable assistance in lending insight and guidance. We further appreciate the willingness of Richard T. Jacobsen of the Center for Applied Thermodynamic Studies at the University of Idaho to share the preliminary results of his work with us.

References

[1]Johnson, R. C., "Real-Gas Effects in Critical-Flow Through Nozzles and Tabulated Thermodynamic Properties," NASA TN-D-2565, 1964.

[2]Jacobsen, R. T., Stewaart, R. B., Penocello, S. G., and McCarty, R. D., "An Interim Thermodynamic Property Formulation for Air," *Fluid Phase Equilibria*, Vol. 37, Elsevier, Amsterdam, 1987, pp. 169–184.

[3]Jacobsen, R. T., "A Revised Interim Thermodynamic Property Formulation for Air," Report on NBS Purchase Order No. 40RANB7B8387, Aug. 1987.

[4]Blanke, W., "Messung, der thermischen Zustandgrössen von Luft im Zweiphasengebiet und seiner Umgebung," Ph.D. Dissertation, Ruhr Univ., Bochum, Federal Republic of Germany, 1973.

[5]Kozlov, A., "Experimental Investigation of the Specific Volumes of Air in the 20°–600°C Temperature Range and 20–700 Bar Pressure Range," Ph.D. Dissertation, Moscow Power Engineering Inst., Moscow, 1968.

[6]Michels, A., Wassenaar, T., Levelt, J. M., and De Graaff, W., "Compressibility Isotherms of Air at Temperatures Between −25°C and −155°C and at Densities up to 560 Amagats (Pressure up to 1000 Atmospheres)," *Applied Scientific Research.*, Sec. A, Vol. 4, No. 143, 1954, pp. 381–392.

[7]Michels, A., Wassenaar, T., Van Seventer, W., "Isotherms of Air Between 0°C and 75°C and at Pressures Up to 2000 Atm," *Applied Scientific Research*, Sec. A, Vol. 4, No. 135, 1954, pp. 52–56.

[8]Romberg, H., "Neue Messungen der thermischen Zustandsgrössen der Luft bei tiefen Temperaturen und die Berechnung der kalorischen Zustandsgrössen mit Hilfe des Kihara Potentials," Verlag des Vereins Deutscher Ingenierore, *Forschungsheft*, Vol. 543, Dusseldorf, 1971.